Scientific Journal of Astana IT University
ISSN (P): 2707-9031 ISSN (E): 2707-904X
VOLUME 10, JUNE 2022

DOI: 10.37943/EOQD2512

D. Nazyrova
Doctoral Student
dilya86@mail.ru, orcid.org/0000-0002-1148-4480
L.N. Gumilyov Eurasian National University, Kazakhstan

Z. Aitkozha
Doctor of Physical and Mathematical Sciences, Associate Professor of the Department of Information Systems
Aitkozha_zh@mail.ru, orcid.org/0000-0002-1213-5186
L.N. Gumilyov Eurasian National University, Kazakhstan

APPLICATION OF MULTISPECTRAL IMAGES TO SEARCH FOR CONSTRUCTION OBJECTS ON THE SPECTRAL SIGNATURES BASE

Abstract: The work is devoted to the study of Landsat-8 multispectral images of not high resolution using the spectral angle method on the base of spectral signatures libraries to detect objects under construction in an urban area. The physical basis of the research method is that all objects have different reflection coefficients depending on the wavelength. This property makes it possible to identify various substances by their spectral signatures. In the work, an automatic comparison of the curves of the spectral reflectivity of objects on a low-resolution space multispectral image was made to identify the identity of the characteristic energy absorption and reflection zones for detecting objects in the construction process. The article also describes the stages of image preprocessing, cross-track illumination correction of the image, atmospheric correction, and mathematical operations of bands transformation, which provide more opportunities for analysis and recognition of objects using a spectral study of a space image. The study accurately determines the presence or absence of the desired materials, since the search is based on the molecular structure of the substance. Also, the use of multispectral images allows you to analyze the entire city at the same time. The initial data was taken from a 2021 Landsat-8 satellite image with 11 bands, with a resolution of 30 meters, which was enhanced to 15 meters during pre-processing. The results of the search and detection of objects under construction in the city are given. The detection results can be used as input data for further in-depth analysis.

Keywords: spectral signature, spectral curve, spectral library, remote sensing, multispectral image, construction objects recognition

Introduction

At present, the construction of new residential and non-residential facilities is being actively carried out in many cities of Kazakhstan. Construction momentum is gaining more and more speed every day. Often the appearance of urban areas is changing beyond recognition. First of all, active construction helps to solve the problem of population growth and demographic development, contributes to the development of urban infrastructure, the transport network, and leads to the modernization and design of new engineering communications. Therefore, the control and monitoring of construction processes, and mapping them for the purpose of visualization and geospatial analysis is an important and urgent task. In the article, it is proposed a method based on spectral features of the reflectivity of the building material on multispectral images to search for construction objects. During pre-processing, the image

DOI: 10.37943/EOQD2512

quality was significantly improved, and the image resolution was increased from 30 to 15 meters. The contribution of this study is to provide a method for efficiently extracting essential information about the objects under construction in the urban areas.

Spectral signature library

The spectral signature or spectral curve is the difference in the reflectivity of objects relative to wavelengths. For any material, the amount of solar radiation which reflected, absorbed or transmitted is varies with wavelength [1]. Fig. 1 shows the spectral curve for structural concrete and is a graphical representation of the relationship between long wavelength and its reflectance values. On the X axis there are the wavelengths at which the reflection coefficients were measured in micrometers. On the Y axis there are the values of the reflection coefficients in the considered zones of the spectrum in fractions of a unit.

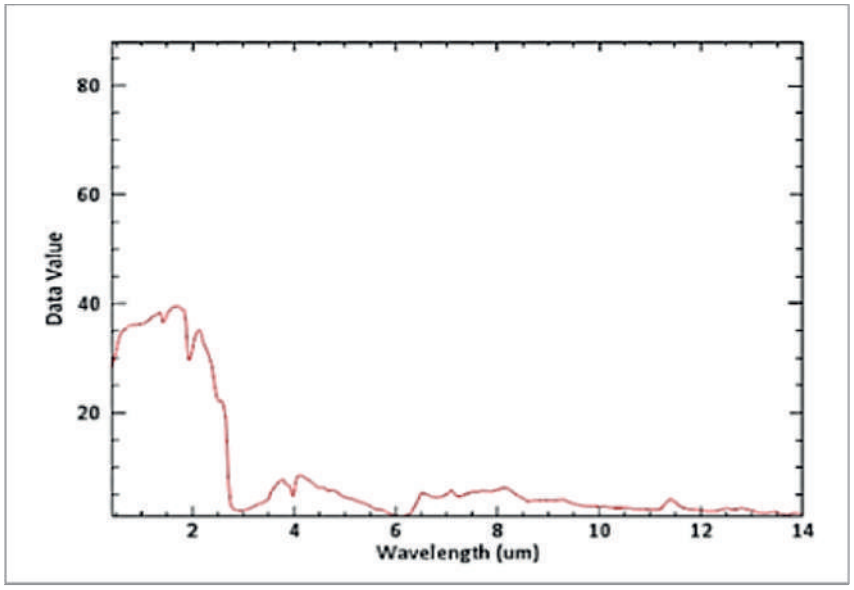

Figure 1. Spectral curve of structural concrete

Spectral libraries are the sets of such graphs-curves of the spectral reflectivity of different objects, obtained by multiband spectrometers in the field or laboratory conditions [2]. The Atlas of Spectral Reflection Curves of Natural Formations, compiled by L.E. Krinov in 1938, can be considered as a prototype of modern spectral libraries. The work published in 1947 contains data on the spectral reflectivity of forest plantations, shrubs, grass cover, mosses, field and garden crops, soils, and artificial materials in various natural zones. To date, there are several public spectral libraries: USGS Digital Spectral Library, JPL (Jet Propulsion Lab) spectral library, Johns Hopkins University Spectral Library, ASTER spectral library, IGCP264 Spectral Library. Two libraries of spectral signatures were used in the study: USGS Digital Spectral Library and ASTER spectral library.

USGS Digital Spectral Library is a library created by USGS Spectroscopy Lab's (current version splib06a - September 2007). It contains data on the spectral reflectance of minerals, rocks, soils, liquids, volatile compounds, frozen volatile compounds, vegetation, artificial materials in the range from 0.2 to 150 micrometers. Contains over 1300 spectral curves.

ASTER spectral library (current version 2.0 - December, 2008) was mainly created to support the use of Terra/ASTER images. It contains data from almost all spectral libraries listed above. In total, it contains more than 2400 spectral curves of natural and artificial materials in the range from 0.4 to 15.4 micrometers.

Scientific Journal of Astana IT University
ISSN (P): 2707-9031 ISSN (E): 2707-904X
VOLUME 10, JUNE 2022

One of the most significant works in the field of application of spectral signature libraries and the Spectral angle mapper method is the work of Kruse et al. where there was determined the fact that it exhibits insensitivity to the effects of illumination and albedo. These distortions may occur due to shadows on the object or roof covering to the side or aside from the observed sensor, factors that have a great influence on sunny weather. Dark and bright illuminated pixels are treated equally, with darker pixels being situated nearer the origin than brightly illuminated pixels. The angle distance to the vector of the training class spectrum will stay the same, meaning that a pixel of the same material under different illumination conditions will most likely be classified in the same class [3]. Zhuokun Pan et. al used the spectral signature library and the spectral angle method to witness short-term urban land use changes. The method received an overall accuracy of 78% and results revealed land use conversions due to the removal of old buildings and their replacement by new construction [4]. Stephanie Brand et. al make an extensive comparative analysis of the spectral angle method with other methods for roof surface classification and to derive a detailed map of roof materials and revealed a significant advantage of this method in comparison with others [5].

Preliminary processing

The use of spectral library data to identify objects requires compliance with a number of mandatory requirements. such as pre-treatment. Pre-processing is the correction and enhancement of satellite images [6]. First of all, this is the elimination of the influence of the atmosphere, on which the final result largely depends. The algorithm of the image pre-processing process is shown in Fig. 2.

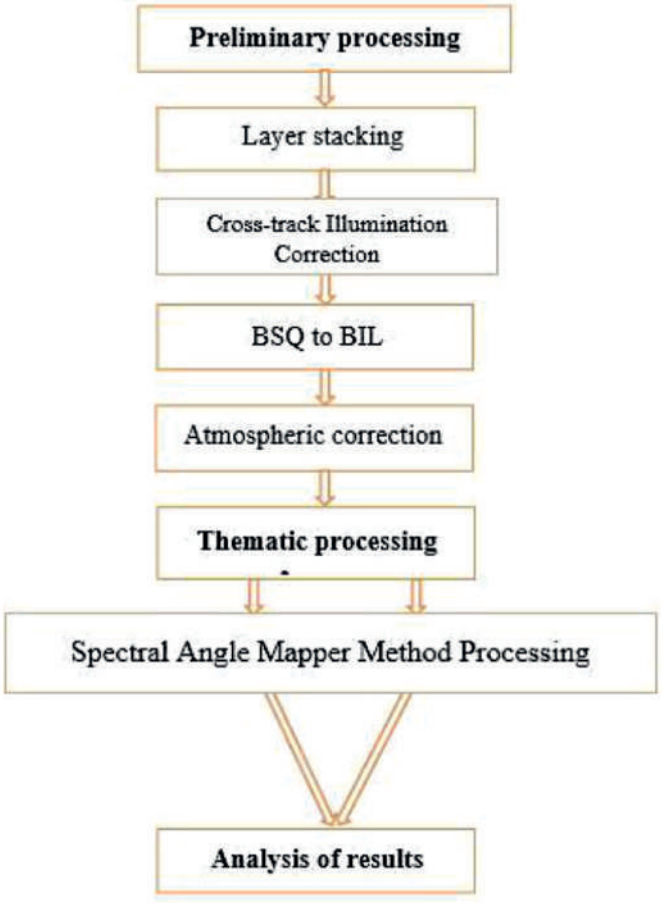

Figure 2. Algorithm of the preprocessing

DOI: 10.37943/EOQD2512

Landsat-8 uses three high-precision astro sensors (ar-3, two of which are active), a Scalable Inertial Reference Unit (SIRU), GPS receivers, and two three-axis magnetometers to optimize the accuracy of satellite orientation. The instruments measure 4096 different levels of reflected light.

Table 1. Characteristics of Landsat-8 Bands

Band 1 – Coastal Aerosol (Coastal / Aerosol, New Deep Blue)	0.433 – 0.453	30 m
Band 2 – Blue	0.450 – 0.515	30 m
Band 3 – Green	0.630 – 0.680	30 m
Band 4 – Red	0.630 – 0.680	30 m
Band 5 – Near Infrared (NIR)	1.560 – 1.660	30 m
Band 6 – Near IR (Short Wavelength Infrared, SWIR 2)	1.560 – 1.660	30 m
Band 7 – Near IR (Short Wavelength Infrared, SWIR 3)	2.100 – 2.300	30 m
Band 8 – Panchromatic (PAN)	0.500 – 0.680	15 m
Band 9 – Cirrus (Cirrus, SWIR)	1.360 – 1.390	30 m
Band 10 – Thermal Infrared (TIRS) 1	10.30 – 11.30	100 m
Band 11 – Thermal Infrared (TIRS) 2	11.50 – 12.50	100 m

Since the initial data are several files, each of which displays a certain part of the spectrum the bands were merged, and a single multiband file was created. All 8 bands as a result of this operation were brought to the same resolution and projection. This process is shown in Fig. 3.

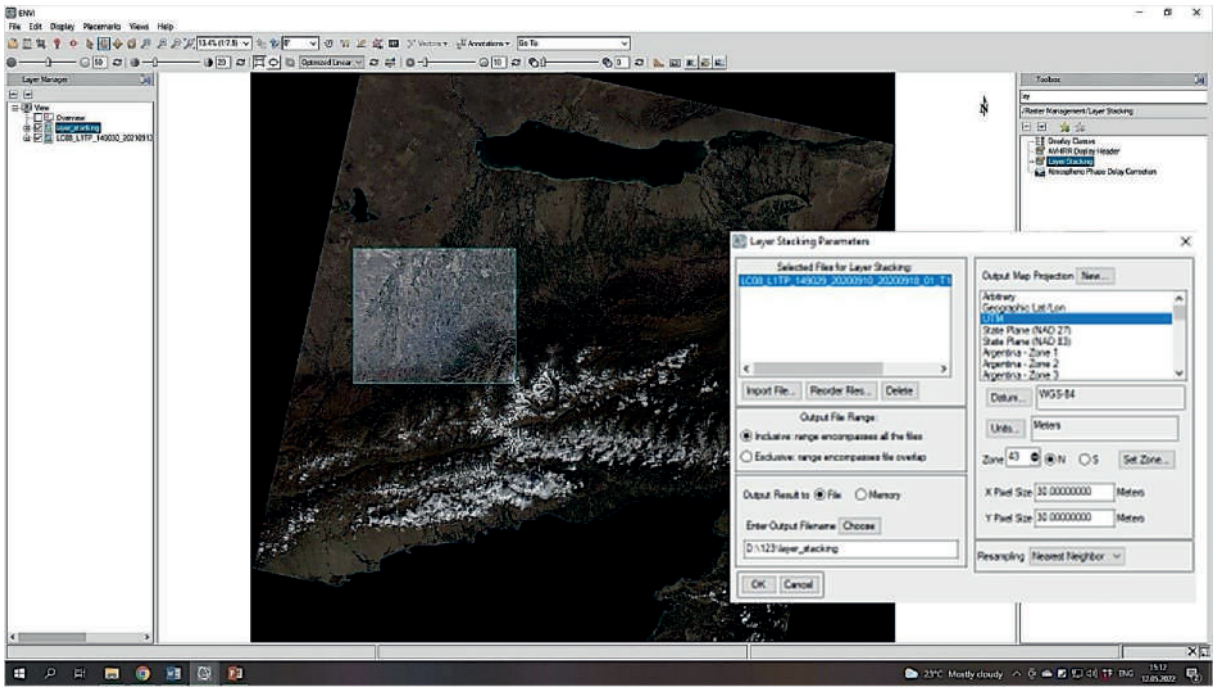

Figure 3. Layer Stacking process

Deviations in the transverse illumination of the image may occur due to the effect of vignetting, scanning errors, or other uneven lighting effects [7]. Therefore, a procedure for transverse illumination correction or Cross-track correction was carried out. The average illumination values along the route were calculated. Then a graph based on the data was plotted to show the average change in the illumination values in the transverse direction. And then the average value and the elimination of variations were calculated using a polynomial function. It is best to use a low order polynomial not to remove local variations in the data.

Scientific Journal of Astana IT University
ISSN (P): 2707-9031 ISSN (E): 2707-904X
VOLUME 10, JUNE 2022

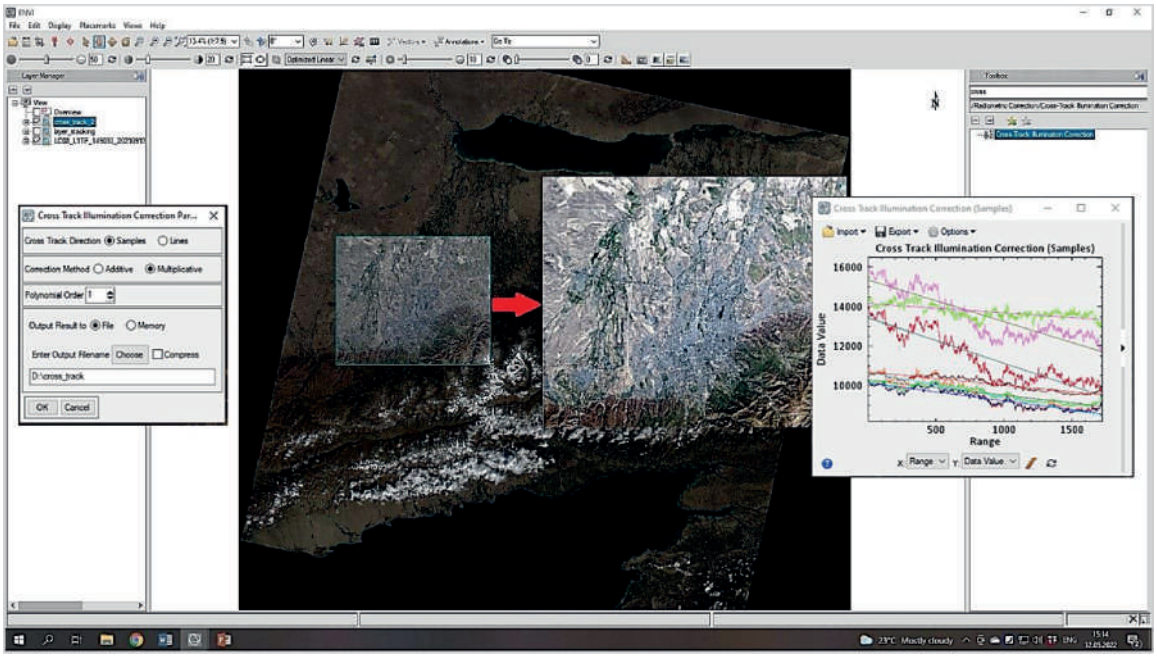

Figure 4. Cross-Track Illumination Correction

The three main ways to organize data in multiband images are band separation by line (BIL), spectral band recording by pixel (BIP) and band recording (BSQ). BIL, BIP and BSQ are not image formats, they are methods of writing pixel values to a file. These files support the display of single and multiband images and can store black and white, grayscale, pseudocolor, full color, and multispectral image data. BIL, BIP and BSQ files are binary and must have an associated ASCII header. This header file contains ancillary information about the image, such as the number of rows and columns, the presence of a color map, and latitude and longitude. The BSQ format is optimal for accessing the spatial information of an image. The BIP format is optimal for accessing the spectral information of an image. The BIL format is basically a compromise format that allows fairly easy access to spatial and spectral information. The format change is shown in Fig. 5.

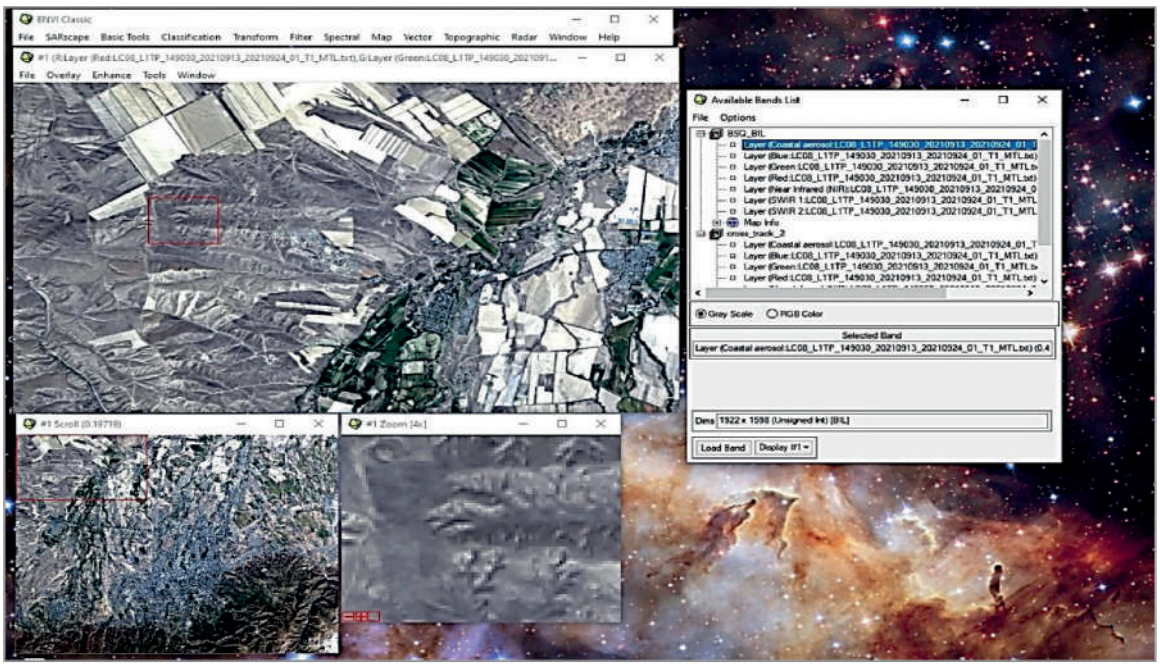

Figure 5. Converting BSQ format to BIL

DOI: 10.37943/EOQD2512

Atmospheric correction (QUick Atmospheric Correction - QUAC) is a very important task of image pre-processing. This tool calculates image correction parameters based only on the information contained in the image without requiring the parameters of the atmosphere model [8]. Working with the QUAC tool is shown in Fig. 6.

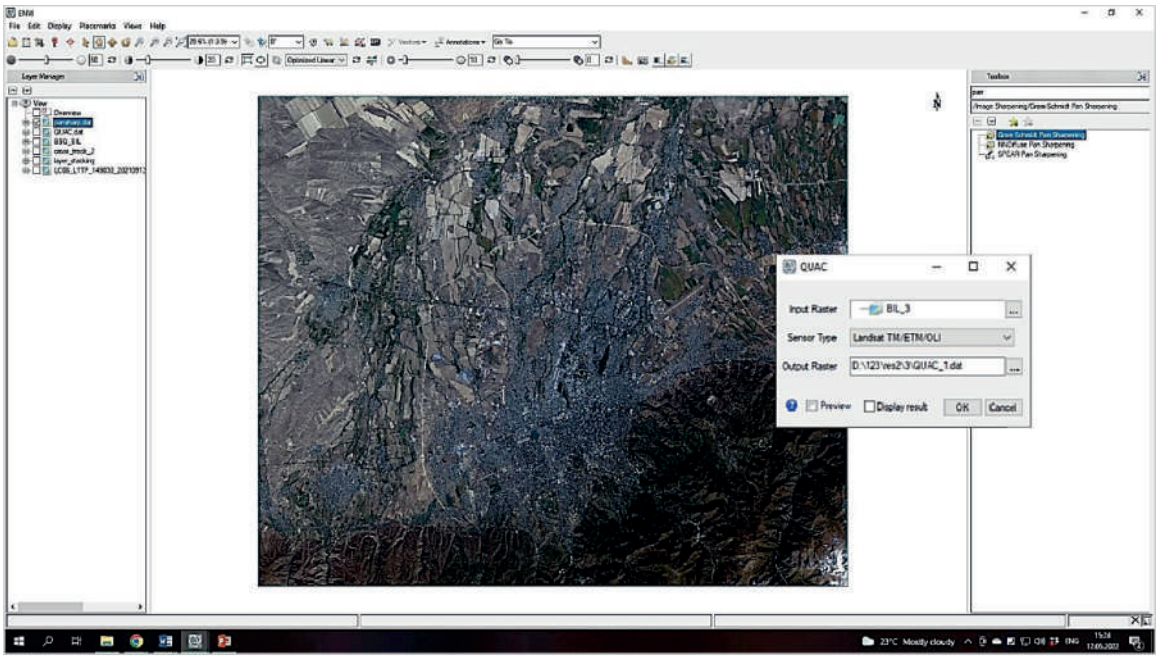

Figure 6. QUick Atmospheric Correction

Panchromatic sharpening is a process that allows you to get one image from the panchromatic and multispectral bands of two products. The panchromatic band, as a rule, has a higher spatial resolution, while the multispectral band has a lower one. Band fusion results in a high-resolution color image [9]. Thus, as a result of this operation, it was possible to improve the image resolution from 30 m to 15 m by merging the two channels, as shown in Fig. 7.

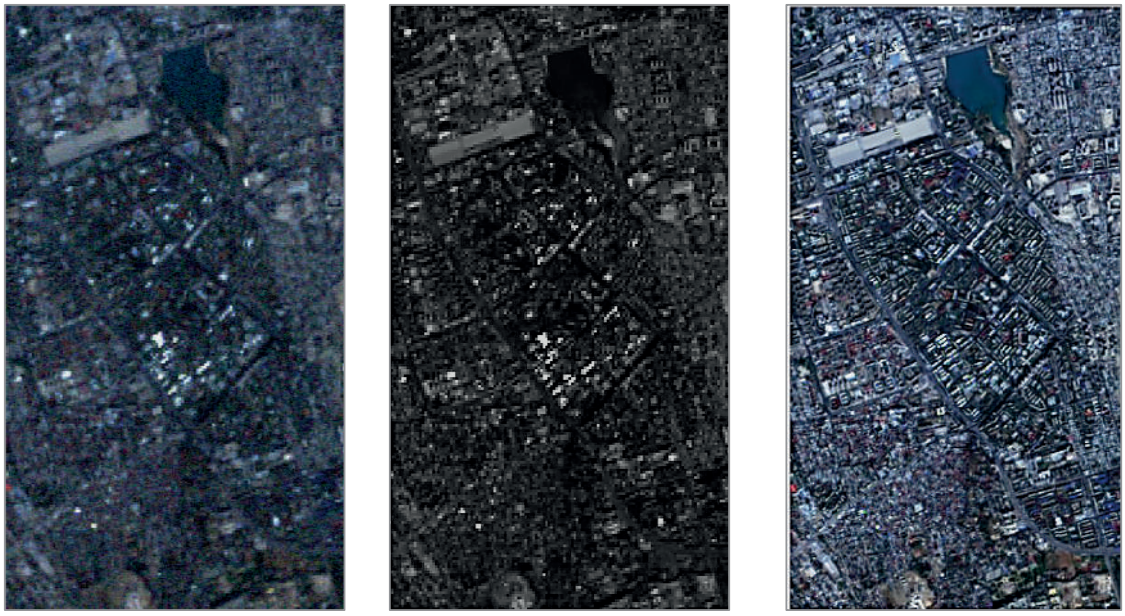

Figure 7. Image resolution enhancement using the Pan-sharpening procedure

Scientific Journal of Astana IT University
ISSN (P): 2707-9031 ISSN (E): 2707-904X
VOLUME 10, JUNE 2022

The pre-processing phase for this work is finished at this stage. Much needed results were obtained to improve the quality and resolution of the image for further work. Satellite sensors are sensitive and dependent on atmospheric conditions, so pre-processing is an extremely important step in the data processing. The difference between the original and corrected spectral profile, as practice shows, is significant and may affect subsequent results.

It is also important to consider the same spectral range and data resolution during pre-processing. The spectral range and resolution of the libraries correspond to the characteristics of the spectrometer. The spectral range of most spectrum libraries is from 0.2-0.4 to 14-25 micrometers with a resolution of 1 to several nanometers. Thus, the library may contain several hundred or even thousands of points to build one curve. The spectral resolution of multizonal imaging systems is not comparable to such data. For example, Landsat7/ETM+ 1,2,3,4,5,7 bands, range 0.45-2.35 micrometers, resolution 65-270 nanometers [10]. Therefore, it is necessary to recalculate the range and resolution of the spectral library for the imaging system.

Spectral angle method (SAM)

The Spectral Angle Mapper (SAM) algorithm is based on an ideal assumption that a single pixel of remote sensing images represents one certain ground cover material and can be uniquely assigned to only one ground cover class. The SAM algorithm is simply based on the measurement of the spectral similarity between two spectra. The spectral similarity can be obtained by considering each spectrum as a vector in q -dimensional space [11], where q is the number of bands. Using the SAM algorithm, it can be detected the spectral similarity of two spectra by calculating the angle between the two spectra, considering them as vectors in space with a dimension equal to the number of bands.

Spectroscopy measures the radiant intensity and energy of the interaction between light and matter to determine its molecular structure. In absorption spectroscopy, the compound that interacts with light behaves as a passive element. It absorbs some of the emitted photons depending on their wavelength, to form the so-called spectral signature. The light which is not absorbed can be transmitted through the sample of the compound or diffusely reflected on it. Once the spectrum of the diffuse reflectance is obtained, it must be processed for the material identification, classification, or discrimination. These are depicted in [12].

Given a pixel spectral set of remote sensing image as $\mathbf{X} = \{\mathbf{x}_1, \mathbf{x}_2, \ldots, \mathbf{x}_n\} \subset \mathbf{R}^q$, the reference spectral set $\mathbf{r} = \{\mathbf{r}_1, \mathbf{r}_2, \ldots, \mathbf{r}_c\} \subset \mathbf{R}^q$, both $\boldsymbol{x}$ and $\boldsymbol{r}$ are the non-zero vector, where $\boldsymbol{q}$ is the number of spectral bands, $\boldsymbol{n}$ is the number of pixels, $\boldsymbol{c}$ is kind of reference spectrum, namely the number of classes in the image. So, the generalized angle (spectral similarity measure) as in [12] $\theta_{c\times n}=\{\theta_{ki}\}$ ($k = 1, \ldots, c$, and $i = 1, \ldots, n$) between the pixel spectra $\boldsymbol{x}_i$ and the reference spectrum $\boldsymbol{r}_k$ is defined as

$$\theta_{ki} = cos^{-1}\left(\langle x_i \times r_k\rangle / (\|x_i\| \times \|r_k\|)\right)$$
$$= cos^{-1}\left(\sum_{j=1}^{q}(x_{ij} * r_{kj}) \;/\; \left(\sqrt{\sum_{j=1}^{q} x_{ij}^2} * \sqrt{\sum_{j=1}^{q} r_{kj}^2}\right)\right) \quad (1)$$

where $\theta_{ki} = \in [0, \pi/2]$, $\langle x_i \times r_k\rangle$ is the inner product of $\boldsymbol{x}_i$ and $\boldsymbol{r}_k$. A pixel spectrum $\boldsymbol{x}_i$ ($i = 1, \ldots, n$) with the minimum or zero spectral angles of the reference spectrum $\boldsymbol{r}_k$ ($k = 1, \ldots, c$) is assigned to the class defined by the reference vector as in [13]. The dissimilarity between species increases with increasing the spectral angle θ_{ki}. So, optimizing the angles between two species increases the classification performance as in [14]. Reference spectrum (endmember spectrum) can be measured from the surface features spectrum, spectral library ASCII file or the mean of the pixel spectral vectors of region of interest in image [15].

DOI: 10.37943/EOQD2512

The search for objects under construction on multispectral images was carried out using the spectral angle method or Spectral Angle Mapper Classification. All pixels of the Landsat-8 multispectral image, including the reference ones, were considered as vectors in the space of spectral features. For the "structural concrete" class, the maximum allowable angle between the reference vector from the library of spectral signatures and the vector of pixels in the image was set equal to 1 rad.

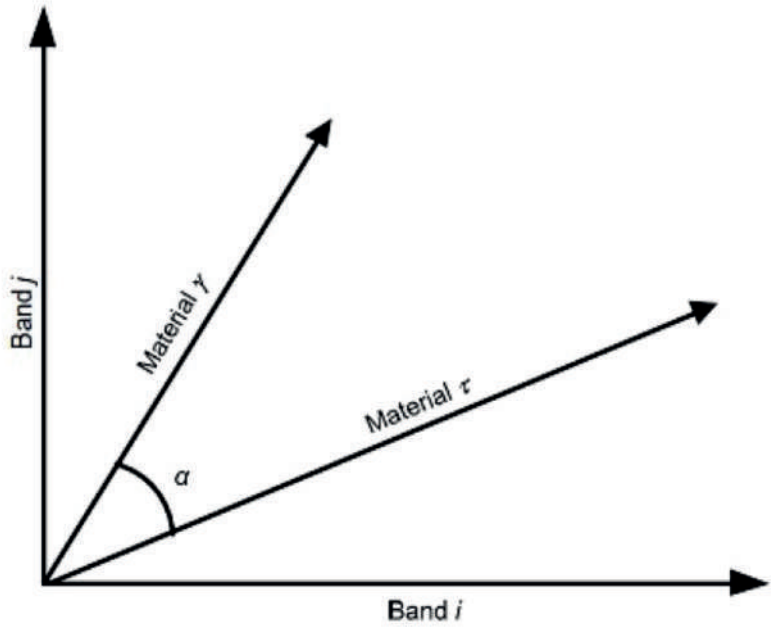

Figure 8. Spectral Angle Method (SAM)

The classification was carried out as follows: if the investigated spectral angle of the multispectral image was less than the maximum, then the pixel belongs to the class "construction concrete slabs", if more, it did not belong, respectively.

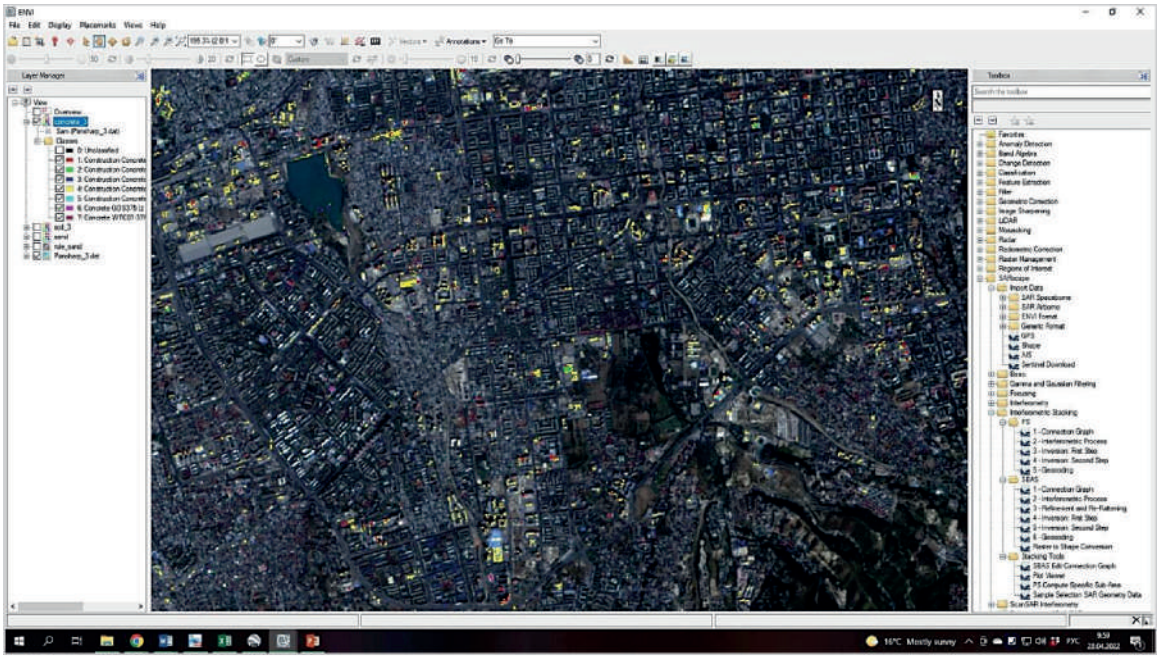

Figure 9. Results of the search by the SAM

Scientific Journal of Astana IT University
ISSN (P): 2707-9031 ISSN (E): 2707-904X
VOLUME 10, JUNE 2022

To check the reliability before starting the search, 10 construction objects in the center of the city were randomly selected in the image.

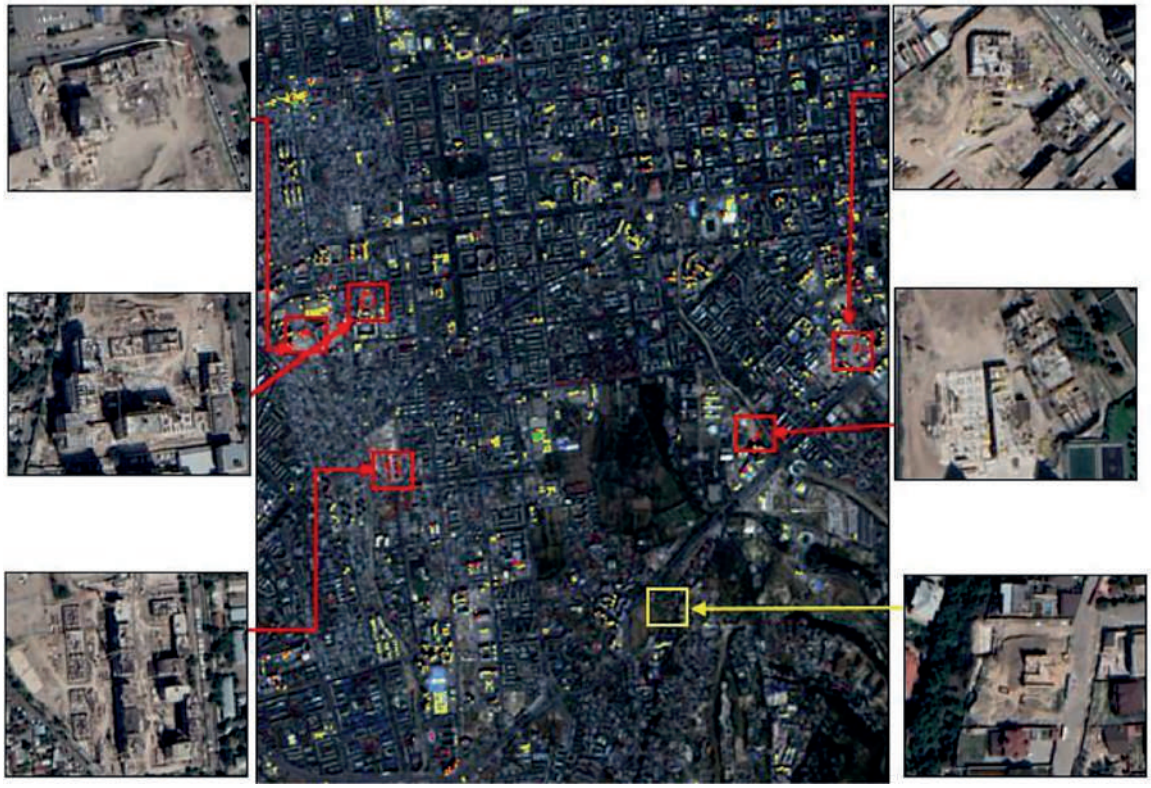

Figure 10. Correspondence of the obtained results with the preliminary sample

As can be seen in the Fig. 10 the area where the spectral signature of building concrete slabs occurs is very extensive. In addition to construction sites where structural concrete is present, concrete roof surfaces and paving slab cases are also highlighted, due to the fact that there is a significant spectral correlation between building materials with similar chemical compositions. Fig. 11 shows the spectral signatures of these materials, similar in composition.

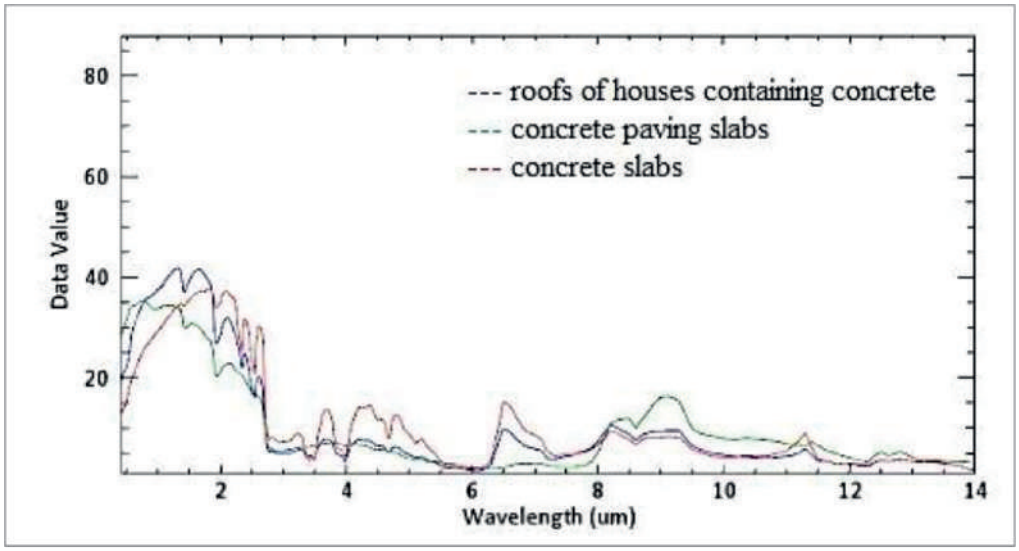

Figure 11. Spectral curves of the roofs of houses containing concrete, concrete paving slabs, building concrete slabs.

It should be noted that concrete is widespread throughout the city. A 2017 building surface materials identification study used hyperspectral imagery as input data [16]. Landsat-8 multispectral images of medium resolution usually have up to 11 bands, and hyperspectral images are almost 20 times larger. However, this problem also arises when using hyperspectral images. This problem is solved by selecting the optimal spectral angle for the SAM method. In our study, changing the angle made it possible to increase the accuracy of the detected objects, although it did not completely eliminate the appearance of false positive results. Nevertheless, it is impossible not to note the fact that among the many illuminated objects of the city, the multi-storey objects under construction of a pre-prepared random sample were completely determined. 5 objects of multi-storey residential buildings under construction were identified, while small houses of the private sector with an area of up to 700 square meters were not highlighted in the image. This may also be due to the not high resolution of the Landsat multispectral image, which is 15 meters. Probably, with increasing resolution, the results will be more accurate. However, this will lead to a significant increase in the cost of work.

Conclusion

In this paper, we analyzed the study of low-resolution multispectral Landsat images using the spectral angle method using spectral signature libraries to detect city objects under construction.

The multispectral Landsat image with a resolution of 15 meters as the initial data showed good results for the search for multi-storey and large objects under construction, while objects of small area were not detected.

Due to the similarity of the chemical composition of building materials, false positive results may also appear in the image. This problem is solved by selecting the optimal spectral angle. However, the investigated area of the search for objects is significantly narrowed and can greatly simplify further data processing. Working with a multispectral image does not require complex processing methods and makes it possible to study a very large area at once without affecting the speed of data processing. When using this method on the basis of low-resolution multispectral images, the brightness values of the pixels are not taken into account, so the results are not affected by the effects of image flare. Since 2009, all satellite images of the Landsat program have been freely available online at https://earthexplorer.usgs.gov [17].

Thus, the use of low-resolution multispectral images gives good results in the search for multi-storey objects under construction using the spectral angle method using libraries of spectral signatures and can be a fast and reliable preliminary assessment method for searching for large construction objects. The detection results can be used as input data for further in-depth analysis.

References

1. Shaw, G.A., & Burke, H.K. (2003). Spectral imaging for remote sensing. *Lincoln laboratory journal*, *14*(1), 3-28.
2. Cherepanov, A. (2009b, August 27). Spectral libraries - sources of data on spectra. https://gis-lab.info/qa/spectrum-lib.html
3. Kruse, F.A., Lefkoff, A.B., Boardman, J.W., Heidebrecht, K.B., Shapiro, A.T., Barloon, P.J., & Goetz, A.F.H. (1993). The spectral image processing system (SIPS)—interactive visualization and analysis of imaging spectrometer data. *Remote sensing of environment*, *44*(2-3), 145-163. https://doi.org/10.1016/0034-4257(93)90013-N

Scientific Journal of Astana IT University
ISSN (P): 2707-9031 ISSN (E): 2707-904X
VOLUME 10, JUNE 2022

4. Pan, Z., Hu, Y., & Wang, G. (2019). Detection of short-term urban land use changes by combining SAR time series images and spectral angle mapping. *Frontiers of Earth Science*, *13*(3), 495-509. https://doi.org/10.1007/s11707-018-0744-6
5. Brand, S. (2011). *Roof surface classification with hyperspectral and laserscanning data: an assessment of spectral angle mapper and support vector machines*. na.
6. Young, N.E., Anderson, R.S., Chignell, S.M., Vorster, A.G., Lawrence, R., & Evangelista, P.H. (2017). A survival guide to Landsat preprocessing. *Ecology*, *98*(4), 920-932. https://doi.org/10.1002/ecy.1730
7. Zhuang, L., & Ng, M.K. (2020, June). Cross-track Illumination Correction For Hyperspectral Pushbroom Sensors Using Total Variation and Sparsity Regularization. In *2020 IEEE 11th Sensor Array and MultiBand Signal Processing Workshop (SAM)* (pp. 1-5). IEEE. doi: 10.1109/SAM48682.2020.9104285
8. Vibhute, A.D., Kale, K.V., Dhumal, R.K., & Mehrotra, S.C. (2015, December). Hyperspectral imaging data atmospheric correction challenges and solutions using QUAC and FLAASH algorithms. In *2015 International Conference on Man and Machine Interfacing (MAMI)* (pp. 1-6). IEEE. doi: 10.1007/978-981-10-3874-7_55
9. Rahaman KR, Hassan QK, Ahmed MR. Pan-Sharpening of Landsat-8 Images and Its Application in Calculating Vegetation Greenness and Canopy Water Contents. ISPRS International Journal of Geo-Information. 2017; 6(6):168. https://doi.org/10.3390/ijgi6060168
10. Young, N. E., Anderson, R. S., Chignell, S. M., Vorster, A. G., Lawrence, R., & Evangelista, P. H. (2017). A survival guide to Landsat preprocessing. *Ecology*, *98*(4), 920-932. doi: 10.1002/ecy.1730
11. Workman Jr, J., & Springsteen, A. (1998). *Applied spectroscopy: a compact reference for practitioners*. Academic Press.
12. Garcia-Allende, P.B., Conde, O.M., Mirapeix, J., Cubillas, A.M., & Lopez-Higuera, J.M. (2008). Data processing method applying principal component analysis and spectral angle mapper for imaging spectroscopic sensors. *IEEE Sensors Journal*, *8*(7), 1310-1316. doi: 10.1109/JSEN.2008.926923
13. Tembhurne, O.W., & Malik, L.G. (2012, February). Hybrid classification using combination of optimized spectral angle mapping algorithm and interpolation method on multispectral and hyper spectral image. In *2012 International Conference on Computing, Communication and Applications* (pp. 1-4). IEEE. doi: 10.1109/ICCCA.2012.6179210
14. Cho, M.A., Debba, P., Mathieu, R., Naidoo, L., Van Aardt, J.A.N., & Asner, G.P. (2010). Improving discrimination of savanna tree species through a multiple-endmember spectral angle mapper approach: Canopy-level analysis. *IEEE Transactions on Geoscience and Remote Sensing*, *48*(11), 4133-4142. doi: 10.1109/TGRS.2010.2058579
15. Liu, X., & Yang, C. (2013, December). A kernel spectral angle mapper algorithm for remote sensing image classification. In *2013 6th International Congress on Image and Signal Processing (CISP)* (Vol. 2, pp. 814-818). IEEE. doi: 10.1109/CISP.2013.6745277
16. Ye, C.M., Cui, P., Pirasteh, S., Li, J., & Li, Y. (2017). Experimental approach for identifying building surface materials based on hyperspectral remote sensing imagery. *Journal of Zhejiang University-SCIENCE A*, *18*(12), 984-990. https://doi.org/10.1631/jzus.a1700149
17. Houska, T. (2012). *EarthExplorer* (No. 136). US Geological Survey.